ISSN 2616-5880 Vol. 3, Issue 1: 51-57, DOI: 10.25236/AJMC.2022.030109

The optical properties of MoSe2 in bulk and monolayer with different crystal orientation based on first-principles calculations

Zhenyang Luo[1,*], Jinge Hao[2], Jialun Li[3]

[1]*School of physics, Changchun University of Science and Technology, Changchun, Jilin, China*
[2]*School of physics and electronic information, Henan Polytechnic University, Jiaozuo, Henan, China*
[3]*College of Science, Nanjing University of Science and Technology, Nanjing, Jiangsu, China*
**Corresponding author*

Abstract: *$MoSe_2$ is a crucial photoelectric functional material with good catalytic activity and two-dimensional layered structure and has a broad application prospect as an essential member of the transition metal chalcogenide (TMDs) family. Different $MoSe_2$ forms have other electronic systems and optical properties. In this paper, based on density functional theory (DFT), bulk $MoSe_2$ and monolayer $MoSe_2$ with different growth directions are taken as research objects to study the band structure, electronic properties, and optical properties of bulk $MoSe_2$ and monolayer $MoSe_2$. According to the calculation results, the band gap of $MoSe_2$ in the (100) crystal direction is the smallest, which can effectively realize ultra-wideband absorption. However, there are significant differences in the dielectric function, absorption coefficient, and reflection coefficient of $MoSe_2$ in the three structures. $MoSe_2$ with different forms has different application fields according to various properties. These results provide reliable data and support for the development of new $MoSe_2$ optoelectronic materials and devices.*

Keywords: *$MoSe_2$; crystal orientation; optical properties; first-principles*

1. Introduction

At present, the development of human society is facing two major challenges: energy and the environment [1]. The development of new energy plays an essential role in the sustainable development of humanity. Among numerous green energy sources such as wind energy, nuclear energy, and solar energy, solar energy, as an inexhaustible, clean new energy, is an effective way to solve the energy problem [2]. Optimizing the use of solar energy so that solar energy for people is a fundamental problem in contemporary science; the mission of developing new photoelectric devices is imminent.

In recent years, $MoSe_2$, as an essential member of the transition metal cognates (TMDs) family, has good catalytic activity and two-dimensional layered structure and is rich in content in the earth's crust. It has attracted more and more attention from researchers in electrochemistry and photocatalysis and is considered a potential photocatalytic material [3]. TMDs have fast electron transfer ability and excellent light absorption performance. There are multiple active sites at the crystal edge of TMDs, which are favorable for photocatalytic reactions [4].

$MoSe_2$, like other TMDs, has a two-dimensional layered structure similar to graphene, identical to the sandwich structure X-M-X (M for Mo element, X for Se element). Van der Waals forces link the layers. Like graphene, different layers of $MoSe_2$ can be detached from the bulk, which causes changes in its band gap, leading to various physical and chemical properties [5]. Similar to $MoSe_2$ in TMDs, $MoSe_2$ has different crystal phase structures of 2H triangular prism D_{3h} and 1T octahedral symmetric O_h, respectively. The former has semiconductor properties, while the latter has metal properties. Similarly, semiconductor materials, bulk materials, and monolayer materials are generally applicable to different application fields due to structural differences. For example, monolayer semiconductor materials can be applied to fiber lasers due to their low loss characteristics. $MoSe_2$ with a bulk structure has a more robust absorption coefficient than the monolayer structure, so it can be used to make absorption devices. Still, its efficiency may be limited by thickness. Although $MoSe_2$ and $MoSe_2$ are widely used, the photoelectronic differences between monolayer and bulk properties of $MoSe_2$ are rarely studied. Therefore, it is essential to look at the electrical and optical properties of bulk $MoSe_2$ and monolayer $MoSe_2$ in theory for their applications in different fields.

ISSN 2616-5880 Vol. 3, Issue 1: 51-57, DOI: 10.25236/AJMC.2022.030109

To further understand $MoSe_2$ and study its electronic structure and optical properties, this paper studies the band structure and electronic and optical properties of $MoSe_2$ and $MoSe_2$ monolayer based on density functional theory (DFT), taking $MoSe_2$ bulk and $MoSe_2$ monolayer as the research object. These results provide reliable data support for the application of $MoSe_2$ in the field of optoelectronics.

2. Computational methods

All the calculations in this work are based on density functional theory, and the Cambridge Serial Total Energy Package (CASTEP) module in Materials Studio is used to complete the required calculations [6]. For $MoSe_2$, the core electron Se: [Ar] is represented with an ultra-soft pseudopotential to better describe the wave function. The exchange-correlation effect of valence electrons (O: 2S22P4, S: 3S2 3P4, Se: 4S2 4P4, Te: 5S2 5P4, Bi: 6S2 6P3) is described by the PBE function in the generalized gradient approximation (GGA). For the Monkhorst -- Pack method of irreducible Brillouin region, the k-point sampling grid is 9 × 9 ×2. A 20 × 20 × 192 grid is used for a fast Fourier transform. TPSD is specified as the minimization algorithm for lattice optimization (the convergence criteria are set as follows: the force acting on the atom is less than 0.03 eV/ Å, the stress is less than 0.05 GPa, the atomic displacement is more minor than 1×10^{-3} Å, and the total energy change per atom is more petite than 1×10^{-5} eV. Gaussian broadening is applied to the eigenvalues calculated from CATEP. Based on the optimized crystal structure, the electronic structure and optical properties of $MoSe_2$ were further calculated. All The preliminary models were obtained from The Inorganic Crystal Structure Database (ICSD). Based on the above parameters, the initial model's atomic position and structure size were optimized, and the stabilized bulk $MoSe_2$ was obtained after reaching the convergence criteria.

3. Results and discussions

3.1. Crystal structure

The crystal structure of $MoSe_2$ is shown in Fig 1. $MoSe_2$ is Molybdenite structured and crystallizes in the hexagonal $P6_3/mmc$ space group. The structure is two-dimensional and consists of two $MoSe_2$ sheets oriented in the (0 0 1) direction. Mo^{4+} is bonded to six equivalent Se^{2-} atoms to form distorted edge-sharing $MoSe_6$ pentagonal pyramids. All Mo–Se bond lengths are 2.55 Å. Se^{2-} is bonded in a 3-coordinate geometry to three equivalent Mo^{4+} atoms.

$MoSe_2$ of the initial structure is optimized based on the optimization criteria described in the previous section. The lattice constants before and after optimization are shown in Table 1. The optimized lattice constants are consistent with those of ICSD: a =3.327 Å, b =3.327 Å, c =33.175 Å, indicating that the calculating method can reliably obtain accurate calculation results $MoSe_2$.

Table 2: The lattice constants of $MoSe_2$ in optimization.

Structures / Lattice constants(Å)	Before optimization	After optimization	Bulk
a	3.327	3.3273	3.3269
b	3.327	3.3273	3.3269
c	33.175	33.175057	33.177135

The structure of monolayer $MoSe_2$, shown in Fig 1, is composed of X-M-X, similar to the sandwich structure. X is the upper and lower layers of Se atoms, and M is the layer of Mo atoms sandwiched in the middle. Strong Mo-Se bonds are formed between atoms in the layer in the form of covalent bonds. The two adjacent layers are combined with A weak van der Waals force, and the layer spacing is about 6.5 Å. For modeling monolayer $MoSe_2$ with (100) and (001) crystal orientation, firstly, relying on the optimized bulk $MoSe_2$ in the above step, the cleave Surface tool in Materials Studio was used to slice the different crystal faces. Eventually, the vacuum layer was established. To effectively avoid the interaction between layers, A large enough vacuum layer needs to be set. In this paper, the thickness of the vacuum layer is set at 15 Å.

ISSN 2616-5880 Vol. 3, Issue 1: 51-57, DOI: 10.25236/AJMC.2022.030109

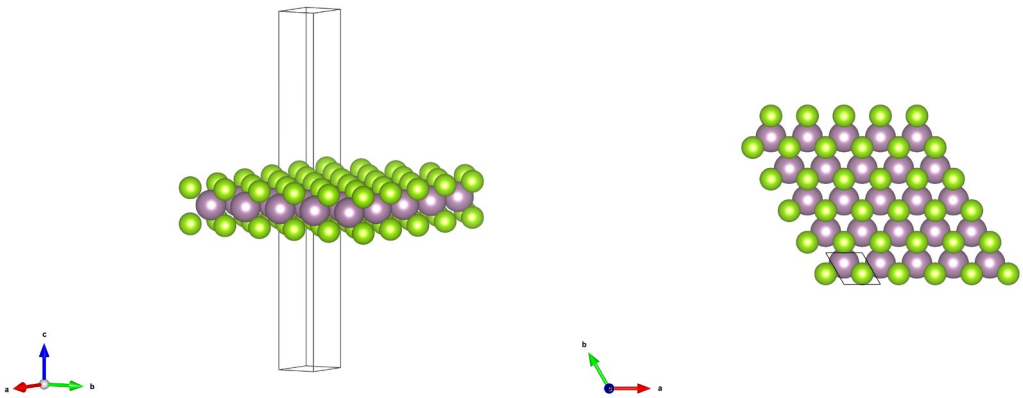

Figure 1: The crystal model of $MoSe_2$ with different crystal structures. Purple spheres represent Mo atoms and green spheres represent se atoms.

3.2. Band structure

In solid-state physics, the band structure is caused by the diffraction of quantum dynamical electron waves in a periodic lattice, which describes the energies that prohibit or allow electrons to carry. The band structure determines many physical properties, especially its electronic and optical properties.

To compare the electronic structures of monolayer $MoSe_2$ (crystalline orientation (001) and (100)) and bulk $MoSe_2$, we calculated their band structures, respectively, as shown in Fig 2. The valence band top (VBM) and conduction band bottom (CBM) of monolayer $MoSe_2$ with bulk $MoSe_2$ and (001) crystal orientation are both located at the high symmetry point H, which indicates that bulk $MoSe_2$ and monolayer $MoSe_2$ (001) exhibit the properties of direct band gap semiconductor. When the valence band electronic guide band transitions, the transition direction displayed on the band diagram is vertical. This means that the momentum of $MoSe_2$'s electrons remains constant during the transition. Conversely, if the conduction electrons fall into the valence band, the rate does not change, and the electron and hole recombination probability is more significant. Therefore, the lifetime of carriers in $MoSe_2$ is often very short, which has the potential to be used in ultrafast optical switches. At the same time, almost all of the energy is emitted as light in this way, which is highly efficient. Therefore, based on this band structure, it is not difficult to find that the bulk system and the monolayer $MoSe_2$ growing along the Z-axis are suitable for making luminescent components. The band gap is the energy difference between the lowest point of the conduction band and the highest valence band. The difficulty of electrons being excited from the valence band to the conduction band increases with the band gap, and the intrinsic carrier concentration and conductivity also decrease with the increase of the band gap. However, (100) crystal-oriented monolayer $MoSe_2$ exhibits the properties of an indirect band gap semiconductor, that is, the valence band top (VBM) and conduction band bottom (CBM) are located at different high symmetry points, and the carrier transition requires phonons to assist. According to the results of the first-principles calculation, the band gap of bulk $MoSe_2$ is 1.42 eV, which is very consistent with the parameters in ICSD (Eg=1.43 eV), proving the accuracy of the analysis. The band gap of monolayer $MoSe_2$ (001) is 1.39 eV, slightly smaller than that of bulk $MoSe_2$, indicating the conductivity of monolayer $MoSe_2$ (001) is somewhat higher than that of bulk $MoSe_2$. The band gap of (100) crystalline monolayer $MoSe_2$ is much smaller than that of z-axis monolayer $MoSe_2$, and its band gap is 0.29 eV. In addition, with a narrow band gap, both monolayers and bulk $MoSe_2$ structures can achieve good absorption from visible to near-infrared regions, indicating that all three $MoSe_2$ types are suitable for photoelectronic applications.

ISSN 2616-5880 Vol. 3, Issue 1: 51-57, DOI: 10.25236/AJMC.2022.030109

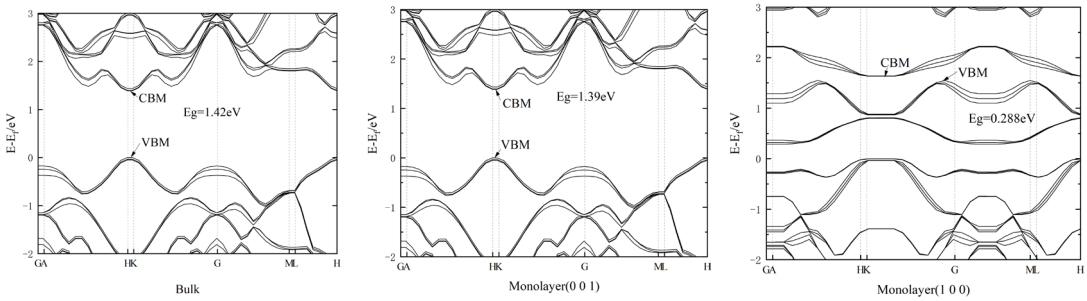

Figure 2: The calculated band structures of $MoSe_2$ with three crystal structures

3.3. The density of states

The density of states is an essential concept in solid physics. The thickness of forms of crystals reflects the chemical bonding mechanism of crystals. Fig 3 shows the total density of states (DOS) and local partial DOS of bulk $MoSe_2$ and monolayer $MoSe_2$ (001) and monolayer $MoSe_2$ (100), respectively, to study the potential chemical bonding mechanism of the $MoSe_2$ molecule. Similarly, the Fermi level is set to 0, represented by a flat line.

In general, the peaks and characteristics of DOS of $MoSe_2$ with three structures show obvious similarity and particularity.

Bulk $MoSe_2$ and (001) crystalline monolayer $MoSe_2$: First of all, all have a deep energy level, mainly composed of Se-4s electronic states. Secondly, the top of the valence band is mainly composed of Mo-4d electronic states and Se-4s electronic states, and se-4p electronic states also contribute a little; The conduction band consists of one part, and the bottom of the conduction band is mainly composed of Mo-4d electron states and Se-4s electron states. The Mo-4d and Mo-4p electronic states contribute more to the bottom of the valence band, while the Se-4s and Se-4p electronic states contribute more to the top of the conduction band. Thirdly, the Fermi energy level of bulk $MoSe_2$ and monolayer $MoSe_2$ (001) is 0, showing prominent nonmetallic properties.

(100) crystalline monolayer $MoSe_2$: First of all, it has no deep energy level. Secondly, the top of the valence band and the bottom of the conduction band are mainly composed of Mo-4d electronic states and Se-4s electronic states. Mo-4d at the bottom of the conduction band contributed the most, and Se-4s at the top of the valence band contributed the most. The electrons in the lower energy region of the Fermi level are the primary bonding electrons, so the total density of states between -5 eV and 0 eV of each phase is further integrated. The average number of bonding electrons per atom of monolayer $MoSe_2$ with (001) and (100) crystal orientation is 2.2006, 2.1956, and 2.7826, respectively. For a stable crystal, the more interactions between atoms, the more bonding electrons [7]. Therefore, the (100) crystalline monolayer $MoSe_2$ has the best structural stability, followed by bulk $MoSe_2$ and (001) crystalline monolayer $MoSe_2$.

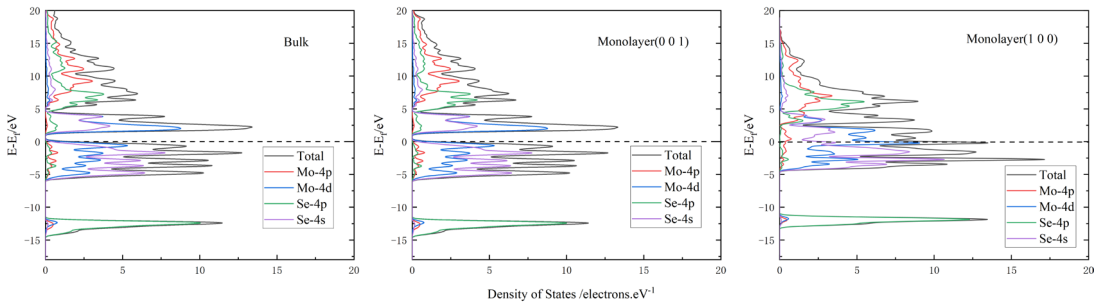

Figure 3: The calculated total and partial density of states of $MoSe_2$ in different crystal structures.

3.4. The dielectric function

$MoSe_2$ is a typical dielectric. The dielectric properties of crystals are analyzed experimentally by

ISSN 2616-5880 Vol. 3, Issue 1: 51-57, DOI: 10.25236/AJMC.2022.030109

measuring the response of materials to electric field stimulation. The stimulus is essentially the time-varying frequency response of the electric field, the polarization or permittivity, so the permittivity measured under the alternating electric field is called the "dynamic permittivity." It is essential to discuss dynamic permittivity because its magnitude is strongly correlated with the measurement frequency. The calculation of the dielectric function of $MoSe_2$ is of great significance in understanding the relationship between the dielectric constant of $MoSe_2$ and the frequency under the action of the time-varying electromagnetic field.

The complex permittivity is usually calculated and further used to represent other properties when calculating optical properties. The complex permittivity ε(ω) is given by the following formula:

$$\varepsilon = \varepsilon_1 + i\varepsilon_2 = N^2$$

Therefore, the relationship between the real and imaginary parts of refractive index and dielectric constant is:

$$\varepsilon_1 = n^2 - k^2$$

$$\varepsilon_2 = 2nk$$

According to the band structure, the calculated real ε_1 and imaginary ε_2 of the dielectric function are shown in Fig 4. By comparing the position of the maximum value of the imaginary part, it is not difficult to find that the $MoSe_2$ of the bulk structure is the same as that of the monolayer $MoSe_2$ of the (001) crystal direction. Still, the peak value of the monolayer $MoSe_2$ of the (001) crystal direction decreases significantly, while that of the monolayer $MoSe_2$ of the (100) crystal direction has a blue shift. We analyze the relative transitions corresponding to these peaks according to the transition rules and heights. For the three forms of $MoSe_2$, the prominent peak of the dielectric function is attributed to the transition between the Se-4p state in the valence band and the Mo-4d state in the conduction band.

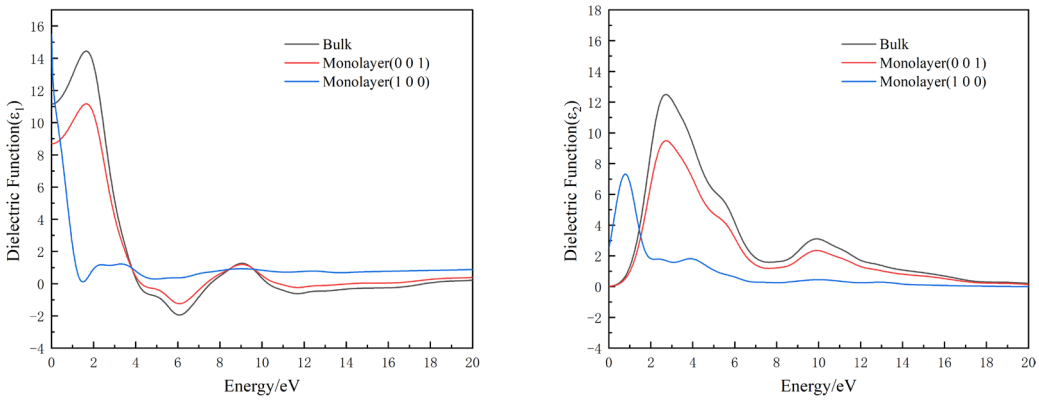

Figure 4: The calculated dielectric functions of $MoSe_2$ in different crystal structures.

3.5. Absorption coefficient

The absorption coefficient is the percentage of energy absorbed per unit length of light passing through an object, usually expressed by alpha. Typically, the absorption coefficient of a material depends on the type of material, but different structures of the same material can also affect the absorption coefficient.

Fig 5 shows the calculated absorption coefficients of three $MoSe_2$ types. For (100) crystal orientation monolayer $MoSe_2$, the infrared absorption capacity is greater than that of bulk $MoSe_2$ and (001) crystal orientation monolayer $MoSe_2$. Therefore, (100) crystal orientation monolayer $MoSe_2$ may be more suitable for making infrared photoelectric detectors. In the visible and ultraviolet regions, bulk $MoSe_2$ has a strong light absorption ability, so it is an excellent choice to use bulk $MoSe_2$ to make ultraviolet and visible light detectors.

ISSN 2616-5880 Vol. 3, Issue 1: 51-57, DOI: 10.25236/AJMC.2022.030109

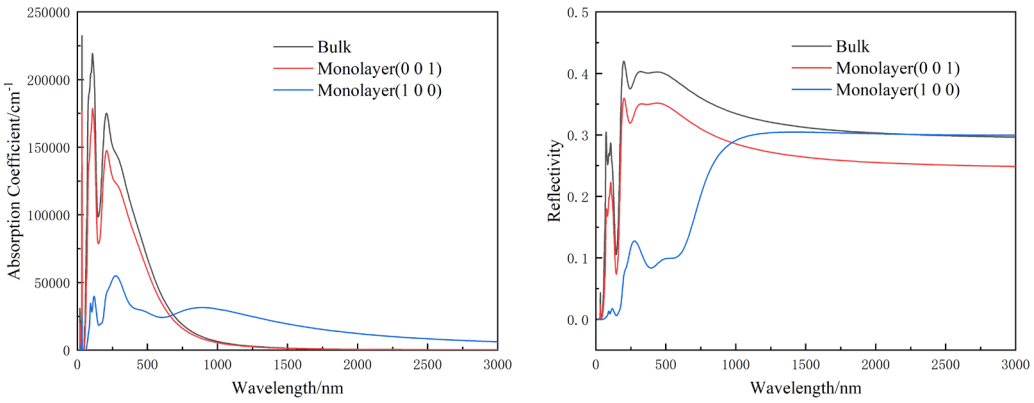

Figure 5: The calculated absorption and reflectivity spectra of $MoSe_2$ in different crystal structures.

3.6. Reflection coefficient

The reflection coefficient is the ratio of the intensity of reflected light from the surface of an object to the power of incident light. The reflection coefficient of the thing is affected by the incident Angle, the intensity of the incident light, and the properties of the object's surface material. Different structures of the same substance have different reflection coefficients, so it is essential to analyze the reflection coefficients of three $MoSe_2$ materials for studying the optical properties of $MoSe_2$.

By matching the electric and magnetic fields on the plane, the reflection coefficient in the simple case of a perpendicular incident on the aircraft can be obtained:

$$R = \left|\frac{1-N}{1+N}\right|^2 = \frac{(n-1)^2+k^2}{(n+1)^2+k^2}$$

Fig 5 shows the calculated spectra of three $MoSe_2$ reflectance coefficients. Bulk $MoSe_2$ and monolayer $MoSe_2$ (001) show promising light absorption regions in ultraviolet and visible light, so they are often used as photocatalysts. In addition, they are also suitable materials for photoelectric devices. For bulk $MoSe_2$ and monolayer $MoSe_2$ (001), the reflection coefficient has a maximum value at wavelengths of 100 nm and 197 nm. The reflection coefficient has a maximum value at the wavelength of 197 nm and a minimum value at 151 nm and 251 nm. When the wavelength is more significant than 465 nm, the reflection coefficient decreases gradually. The reflection coefficient of bulk $MoSe_2$ finally tends to 2.96, and that of monolayer $MoSe_2$ (001) finally tends to 2.49. This suggests that the reflection coefficients of all three $MoSe_2$s are stable and do not mutate in the ultraviolet band, making them suitable for use as optical detectors. The reflection coefficients of bulk $MoSe_2$ are higher than that of monolayer $MoSe_2$ (001) and monolayer $MoSe_2$ (100), indicating that the reflection coefficients of bulk $MoSe_2$ are more significant than that of monolayer $MoSe_2$ (001) and monolayer $MoSe_2$ (100) in both ultraviolet and visible wavelengths. These results indicate that at ultraviolet and visible wavelengths (10 nm-760 nm), bulk $MoSe_2$ has the highest reflection coefficient and can reflect more photons. Monolayer $MoSe_2$ (100) has the lowest reflection coefficient and can absorb more photons. Therefore, the bulk $MoSe_2$ of the three structures is more suitable as an anti-reflective layer.

Due to the difference in crystal structures between bulk $MoSe_2$ and monolayer $MoSe_2$ in (001) direction and monolayer $MoSe_2$ in (100) orientation, their optical properties are also quite different. At the same time, this difference in crystal structure leads to varying interactions between atoms and changes in electronic design. Theoretical calculations show that compared with monolayer $MoSe_2$, the ionic interaction in bulk $MoSe_2$ between Mo atom and Se atom is more substantial, but the covalent interaction is weaker. These data can support novel Se-based energy conversion materials and devices.

4. Conclusion

In this paper, the electronic and optical properties of (001) -oriented monolayer $MoSe_2$ and (100) -oriented monolayer $MoSe_2$ structures are calculated based on the CASTEP module of Materials Studio based on density functional theory. The band gap of $MoSe_2$ in (100) crystal direction is the smallest,

ISSN 2616-5880 Vol. 3, Issue 1: 51-57, DOI: 10.25236/AJMC.2022.030109

which can effectively achieve ultra-wideband absorption. In addition, the differences among dielectric function, absorption coefficient, and reflection coefficient are analyzed. $MoSe_2$ with different structures has different application fields according to various properties. These results provide reliable data and support for the development of new $MoSe_2$ optoelectronic materials and devices.

References

[1] Spasianoa D, Marottaa R, Malato S, et al. Solar photocatalysis: Materials, reactors, some commercial, and pre-industrialized applications. A comprehensive approach [J]. Applied Catalysis B: Environmental, 2015, 170-171: 90–123.

[2] Tong H, Ouyang S, Bi Y, et al. Nano-photocatalytic materials: possibilities and challenges [J]. Advanced Materials, 2012, 24: 229–251.

[3] He W, Cai J, Jiang X, et al. Generation of reactive oxygen species and charge carriers in plasmonic photocatalytic Au@TiO2 nanostructures with enhanced activity [J]. Physical Chemistry Chemical Physics, 2018, 20: 16117–16125.

[4] Guo W, Chen Y, Wang L, et al. Colloidal synthesis of $MoSe_2$ nanonetworks and nanoflowers with efficient electrocatalytic hydrogen-evolution activity[J]. Electrochim Acta, 2017, 231: 69–76.

[5] Chhowalla M, Liu Z, Zhang H. Two-dimensional transition metal dichalcogenide (TMD) nanosheets [J]. Chemical Society Reviews, 2015, 44(9): 2584–2586.

[6] Clark S J, Segall M D, Pickard C J, Hasnip P J, Probert M IJ, Refson K, Payne M C. First principles methods using CASTEP [J]. Zeitschrift fuer Kristallographie, 2005, (220): 567-570.

[7] M. Pekguleryuz, P. Labelle, E. Baril, D. Argo. "Magnesium diecasting alloy AJ62x with superior creep resistance and castability."2003 Magnesium Technology. TMS, San Diego, 2003. 201-207.